THE JOURNAL OF PHYSICAL CHEMISTRY B

Article

pubs.acs.org/JPCB

Correlating Nitrile IR Frequencies to Local Electrostatics Quantifies Noncovalent Interactions of Peptides and Proteins

Pranab Deb, Tapas Haldar, Somnath M Kashid, Subhrashis Banerjee, Suman Chakrabarty,* and Sayan Bagchi*

Physical and Materials Chemistry Division, CSIR-National Chemical Laboratory, Dr. Homi Bhabha Road, Pune 411008, India

Supporting Information

ABSTRACT: Noncovalent interactions, in particular the hydrogen bonds and nonspecific long-range electrostatic interactions are fundamental to biomolecular functions. A molecular understanding of the local electrostatic environment, consistently for both specific (hydrogen-bonding) and nonspecific electrostatic (local polarity) interactions, is essential for a detailed understanding of these processes. Vibrational Stark Effect (VSE) has proven to be an extremely useful method to measure the local electric field using infrared spectroscopy of carbonyl and nitrile based probes. The nitrile chemical group would be an ideal choice because of its absorption in an infrared spectral window transparent to biomolecules, ease of site-specific incorporation into proteins, and common occurrence as a substituent in various drug molecules. However, the inability of VSE to describe the dependence of IR frequency on electric field for hydrogen-bonded nitriles to date has severely limited nitrile's utility to probe the noncovalent interactions. In this work, using infrared spectroscopy and atomistic molecular dynamics simulations, we have reported for the first time a linear correlation between nitrile frequencies and electric fields in a wide range of hydrogen-bonding environments that may bridge the existing gap between VSE and H-bonding interactions. We have demonstrated the robustness of this field-frequency correlation for both aromatic nitriles and sulfur-based nitriles in a wide range of molecules of varying size and compactness, including small molecules in complex solvation environments, an amino acid, disordered peptides, and structured proteins. This correlation, when coupled to VSE, can be used to quantify noncovalent interactions, specific or nonspecific, in a consistent manner.

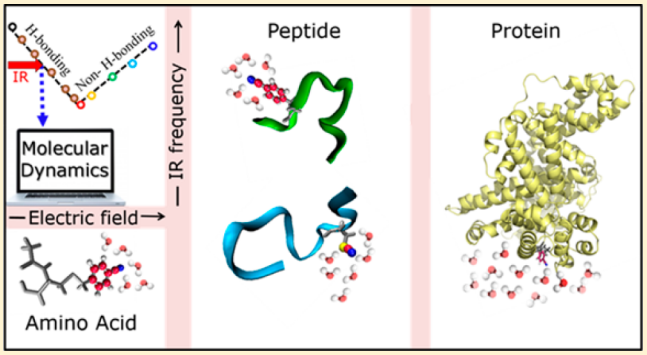

1. INTRODUCTION

Noncovalent interactions, namely hydrogen bonding (H-bonding), electrostatic, van der Waals' interaction, etc. play a crucial role toward biomolecular functions.[1−4] A key challenge is to understand the relative role of these interactions toward processes like molecular recognition, protein folding, and enzyme catalysis within the heterogeneous molecular environments of the proteins and enzymes. Unfortunately, it is extremely nontrivial to define and measure these noncovalent interactions in a microscopic manner using experimental observables. Some of the commonly used descriptors include dissociation constant (K_D), H-bonds, and interactions involving π-electron cloud of the aromatic residues.[1] However, K_D is determined by the overall noncovalent interactions between the interacting species, hence lacks the microscopic insight regarding specific interactions. The H-bonding concepts, mostly defined by arbitrary geometric criteria, do not account for the energetically significant nonspecific interactions.[1] The relative role of various types of noncovalent interactions can also be obtained by decomposing the total interaction energy in terms of the contributing factors like electrostatic interactions, van der Waals' interactions etc., but that requires a theoretical approach involving quantum chemical calculations. However, it has become increasingly evident that the electrostatic interactions play a major role toward biomolecular function.[3−14] Thus, an experimental measurement of the electric field experienced by a probe molecule due to its environment can provide microscopic insight about the local electrostatics of a highly heterogeneous molecular environment typically encountered in biomolecules. Moreover, due to the directionality associated with electric field, it contains more detailed information on the environment as compared to the interaction energy.

Toward achieving this goal, a wide attention has recently been drawn into vibrational Stark spectroscopy (VSS), as infrared (IR) probes are sensitive reporters of the local electrostatic environments.[15−27] IR spectroscopy probes the energy gap ($\bar{\nu}$) between the ground and the first excited vibrational state that depends on the electric field exerted by the environment. Since these states have different dipole

Received: March 16, 2016
Revised: April 19, 2016
Published: April 19, 2016

DOI: 10.1021/acs.jpcb.6b02732
J. Phys. Chem. B 2016, 120, 4034−4046

moments for an anharmonic diatomic IR probe, they are stabilized to different extents by the electric field from the environment depending on the orientation between the dipole and the field. A slight change in the environment modifies the exerted electric field on the IR probe by $\Delta\vec{F}$, thereby causing a shift in the IR transition energy ($\Delta\bar{\nu}$) that is linear with the difference of the dipole moment ($\Delta\vec{\mu}$) of the two vibrational states ($\Delta\bar{\nu} = -\Delta\vec{\mu}\cdot\Delta\vec{F}$). Thus, a linear correlation between IR frequency and electric field would exist in different environments of the IR probe, provided $\Delta\vec{\mu}$ (also known as the Stark tuning rate) is independent of the environment, which has been shown to be the case using VSS.[15,25,28,29] As long as the vibration of the IR probe is local and decoupled from the rest of the molecule, the electric field estimated directly from the IR experiments can serve as a microscopic and quantitative descriptor of noncovalent interactions. Due to this inherent advantage, IR spectroscopy has been performed in recent times on biomolecules labeled with vibrational probes to access the local electric fields in biological macromolecules.[11,30]

One of the numerous IR probes that have been extensively used to estimate electric fields inside proteins is the carbonyl (C═O) probe. Using VSS, it has been experimentally demonstrated that the linear dependence of the C═O stretching frequencies ($\bar{\nu}_{C=O}$) to the electric field is maintained irrespective of the H-bonding status.[1,11,31,32] Using IR/NMR correlations, the electrostatic nature of the C═O hydrogen bonds have been illustrated.[33] However, the intrinsic overlap of $\bar{\nu}_{C=O}$ with the protein backbone IR absorption limits the use of C═O in electric field estimation. A local vibration that absorbs in an uncluttered mid-IR spectral region devoid of any background absorption from the protein and side-chains is the nitrile (C≡N) stretch.[16,30,34−40] Interestingly, C≡N is also a very common substituent in small molecules used as inhibitors, including a remarkable number of drugs currently in use or in clinical trials.[41] Several reports are now available for introducing C≡N probes into proteins.[16,34,36,38−40] These advantages make C≡N an ideal IR probe to investigate protein structure, interactions and dynamics.[13,42−44] However, one unusual characteristic of the group is the shift of the nitrile stretch ($\bar{\nu}_{C\equiv N}$) to higher frequencies (blue-shift) in the IR spectrum upon H-bonding, whereas a red-shift occurs in C═O.[45−49] Thus, for C≡N in H-bonding environment, a drastic departure from the linear field-frequency correlation derived from the vibrational Stark effect (VSE) has been observed.[27,30,40] It has been suggested that, unlike C═O, the H-bonding interactions in C≡N are not purely electrostatic (that involves only the first order Coulomb interactions) and the nonelectrostatic contribution to $\bar{\nu}_{C\equiv N}$ can be attributed to the higher order interactions like polarization and other quantum mechanical aspects of H-bonding interactions.[13,47,49−51] So far this nonelectrostatic contribution has remained a barrier toward the estimation of electric field on C≡N in H-bonding environments, restricting the field measurements only to non-H-bonded C≡N.[47,49−51] This has severely limited the utility of C≡N based IR probes in biomolecules because H-bonds are often critical components of the environment one seeks to characterize. Thus, in order to establish the general utility of C≡N to probe noncovalent interactions, a systematic and quantitative study of the dependence of $\bar{\nu}_{C\equiv N}$ on electric field for H-bonded C≡N is crucial.

Nitriles are generally introduced into biomolecules as thiocyanates (SCN) via cysteine modification (Cys-SCN) or as aromatic nitriles via cyano phenylalanine (p-CN-Phe). It has been reported that benzonitrile (PhCN) and methyl thiocyanate (MeSCN) can serve as model nitriles (proxies) for p-CN-Phe and Cys-SCN, respectively.[30,52] In the present work, we have used IR spectroscopy to obtain $\bar{\nu}_{C\equiv N}$ and atomistic classical molecular dynamics (MD) simulations to estimate the average electric fields ($F_{C\equiv N} = \left\langle \vec{F}\cdot\vec{u}_{C\equiv N}\right\rangle$)[31] exerted on the C≡N bond of PhCN and MeSCN in different solvation environments (both H-bonded and non-H-bonded). The non-H-bonded environments were scanned using neat organic solvents and the H-bonded environments using aqueous binary mixtures. For non-H-bonded C≡N where the interactions are electrostatic, we have observed a linear dependence between $\bar{\nu}_{C\equiv N}$ and $F_{C\equiv N}$ with a positive slope as expected from VSE. This linear correlation is not expected to continue for the H-bonded C≡N due to the nonelectrostatic contribution to the C≡N H-bonding interaction. However, our results demonstrate a new linear dependence between $\bar{\nu}_{C\equiv N}$ and $F_{C\equiv N}$, both for H-bonded PhCN and MeSCN, but with a negative slope which cannot be described by VSE. Combining the H-bonded and non H-bonded environments together we obtain a V-shaped frequency-field correlation diagram, which can now be used to predict the frequency/field at arbitrary environment if the field/frequency is known, respectively.

In order to verify if the field-frequency calibration obtained for H-bonded C≡N in binary solvent mixtures can be extended to other H-bonded C≡N systems, we have performed various stringent tests on molecules of varying sizes, structural compactness and solvation environments. The predicted electric fields on C≡N in different THF/water solutions using the field-frequency calibration of H-bonded nitriles have been compared with that obtained from classical MD simulations. We have also shown the validity of this correlation on small molecule nitriles in the presence of high concentration of a denaturant (urea) in aqueous solution. Furthermore, using the calculated electric fields from MD simulations, we have predicted $\bar{\nu}_{C\equiv N}$ of multiple mutants of two nitrile modified peptides and compared them with the experimental observations. The nitrile groups of these peptides are H-bonded as they have been previously reported to be exposed to the aqueous solvent environment.[53,54] Finally, we have tested our approach for larger biomolecules, namely nitrile modified proteins.

Overall, we have used two different small molecule nitriles that can serve as proxies to the incorporated nitriles in biomolecules and have demonstrated that electric fields can be directly obtained from IR experiments in case of H-bonded C≡N even though these interactions cannot be predicted by VSE. The predictive power of our field-frequency correlation curve was extensively tested on nitrile modified amino acid, disordered peptides and a structured protein system. Our results illustrate that the noncovalent interactions involving C≡N stretch can be estimated from IR experiments in a quantitative fashion, irrespective of the specificity of the interactions.

2. MATERIALS AND METHODS

2.1. Materials. Benzonitrile, methyl thiocyanate, *N*-acetyl cysteine, bovine serum albumin (BSA), and solvents like hexanes, dibutyl ether, tetrahydrofuran (THF), dimethylforma-

DOI: 10.1021/acs.jpcb.6b02732
J. Phys. Chem. B 2016, 120, 4034−4046

mide (DMF), and dimethyl sulfoxide (DMSO) were obtained from Sigma-Aldrich and used without further purification. Urea was purchased from Invitrogen and used as supplied.

2.2. FTIR Spectroscopy. IR absorption spectra were recorded on a FTIR-8300 (Shimadzu) spectrometer with 2 cm^{-1} resolution at room temperature. For each sample, ~60 μL of the sample solution was loaded into a demountable cell consisting of two windows (CaF_2, 3 mm thickness, Shenzen Laser), separated by a mylar spacer of 56 μm thickness. Both the nitriles (PhCN and MeSCN) were dissolved independently in, aprotic solvents, water, water/DMSO, water/DMF, and water/THF binary mixtures, and aqueous urea solutions (5M) so that the final concentration of liquid sample is 10 mM for the IR studies. For recording the IR spectra of nitriles in aprotic solvents, 16 scans were collected whereas 100 scans were recorded for nitriles in water, water/DMSO binary mixtures and aqueous urea solutions. For nitrile mutated amino acid (compound **3**) in water and nitrile mutated BSA (compound **7**) in aqueous buffer 100 scans were collected. A polynomial fit was used to baseline each FTIR absorbance spectrum. The processed absorption spectra were fit to a Gaussian to obtain the reported peak frequencies.

2.3. Computational Methods. Molecular dynamics (MD) simulations were carried out using the GROMACS[55] (version: 4.6.5) software. General AMBER force field (GAFF)[56] was used to model benzonitrile, methyl thiocyanate, and all other nonaqueous solvent molecules. The force field parameters for the solvent molecules were obtained from virtualchemistry.org,[57] a database of parameters and physical properties of a wide range of organic liquids, which have been thoroughly tested and benchmarked for reliability.[58] CHARMM force field parameters[59] were used to model the THF and THF/water binary mixtures, since this combination has been shown to reproduce the temperature dependent miscibility in THF/water binary mixtures.[60] For the simulations involving binary mixtures (water with DMSO/DMF/THF) mixtures, the nonbonded interaction parameters between water and the other solvent molecules were generated using the standard Lorentz–Berthelot mixing rule given by $\sigma_{ij} = \frac{1}{2}(\sigma_i + \sigma_j)$ and $\varepsilon_{ij} = \sqrt{\varepsilon_i \varepsilon_j}$, where σ_i and ε_i are the Lennard-Jones parameters for the individual solvent molecules. Amber ff99SB-ILDN force field was used to model the standard amino acid residues in peptides and proteins.[61] The modified residue p-CN-Phe in the peptide, Mastoparan X, was created by combining the parameters of benzonitrile (GAFF) and PHE residue (Amber ff99SB-ILDN). Similarly the cysteine modified residues in the peptide CM15 and protein BSA were created by combining the parameters of the Cystine residue (Amber ff99SB-ILDN) with those of methyl thiocyanate (GAFF) and modified amino acid (GAFF), respectively. The structure of the BSA protein was obtained from the PDB data bank (ID: 4F5S). The simulations of the Mastoparan X peptide were started from multiple initial conformations including a fully extended conformation in order to rigorously check the equivalence of the calculated average electric field from independent runs. TIP3P water model[62] was used in the simulations involving water molecules.

A single probe molecule (benzonitrile or methyl thiocyanate) was solvated in a cubic box of 5 nm dimension of respective solvent molecules. The solvated system was sequentially processed through (i) energy minimization using steepest descent algorithm, (ii) equilibration in NVT ensemble at 300 K temperature for 100 ps using the velocity rescale thermostat,[63] and (iii) equilibration in NPT ensemble at 300 K temperature and 1 bar pressure (using Parrinello–Rahman barostat[64]) for 1 ns. For the systems involving benzonitrile and methyl thiocyanate in various solvents, the production run was continued for 10 ns, with positions and forces on each atom being saved at every 0.2 ps. For the Mastoparan X and CM15 peptides much longer production runs of 50 ns were used, since the electrostatic field needed to be averaged over various conformations of the peptide. For the protein (BSA) production runs of 50 ns were used starting with different conformations and the average electric field has been calculated from multiple trajectories.

The electric field ($F_{C\equiv N}$) exerted onto the C≡N bond by the environment was calculated by projecting the total electrostatic field due to the rest of the system onto the C≡N bond vector following the same protocol as used in ref 31. The equations used to define ($F_{C\equiv N}$) are the following,

$$\vec{F}_i = \vec{f}_{i,\text{electro}} / q_i$$

$$F_{C\equiv N} = \frac{1}{2}\langle \vec{F}_C \cdot \hat{\mu}_{C\equiv N} + \vec{F}_N \cdot \hat{\mu}_{C\equiv N} \rangle \quad (1)$$

where, $\vec{F}_i$ denotes the electric field and $\vec{f}_{i,\text{electro}}$ denotes the total electrostatic (Coulomb) force exerted on the ith reference atom (C and N atoms of the C≡N bond), and q_i denotes the partial charge obtained from the force field. $\hat{\mu}_{C\equiv N}$ is the unit vector along the C≡N bond. Thus, the reported $F_{C\equiv N}$ values were averaged over both the C and N atoms as well as over the configurational ensemble along the MD trajectory until convergence was achieved. For complete generality and consistent treatment of the electric field, the total exerted electric field was calculated from to the full solvation system.

3. RESULTS AND DISCUSSIONS

3.1. Vibrational Solvatochromism. Solvatochromic experiments provide another alternative to VSS where the electric field on the IR probe can be varied by dissolving the solute in various solvents of varying polarity.[1,11,30−32,40] Different solvents exert different electric fields on the dipolar probe that result in different IR peak frequencies. We have performed solvatochromic IR experiments of PhCN and MeSCN, where different organic solvents of varying polarity serve as the benchmark solvents to elucidate the nature of C≡N group in different electrostatic environments. Further, we have dissolved PhCN and MeSCN in neat water and aqueous binary mixtures of DMSO and DMF with varying cosolvent:water ratio (v/v) to illustrate the sensitivity of the $\bar{\nu}_{C\equiv N}$ in a wide range of H-bonding environments.

3.1.1. Nitriles in Non-H-Bonding Environment. The non-H-bonding solvation environments of C≡N are scanned through a wide range of polarity by dissolving in various solvents having different dielectric constants. The effect of solvent polarity on C≡N is reflected in $\bar{\nu}_{C\equiv N}$ (Figure S1A for PhCN and Figure S1B for MeSCN). In the most nonpolar solvent, hexane, PhCN and MeSCN show peak maxima at 2233.4 and 2164.3 cm^{-1}, respectively. $\bar{\nu}_{C\equiv N}$, gradually decrease (red-shift) in aprotic solvents with increasing solvent polarity. In the most polar aprotic solvent, DMSO, $\bar{\nu}_{C\equiv N}$for PhCN and MeSCN are at 2227.5 and 2154.2 cm^{-1}, respectively. A 5.9 cm^{-1} red shift in $\bar{\nu}_{C\equiv N}$ is observed for PhCN as the solvation environment is changed from hexane to DMSO, whereas MeSCN shows a red-

DOI: 10.1021/acs.jpcb.6b02732
J. Phys. Chem. B 2016, 120, 4034−4046

shift of 10.1 cm^{-1} for the same. The greater red-shift in the case of MeSCN illustrates its greater sensitivity toward solvent polarity as compared with PhCN. This result reinforces the earlier results from VSS, where the sulfur-based nitriles have been found to have a larger $\Delta\vec{\mu}$ than the aromatic nitriles.[30,40] However, the overall red-shifting trend in non-H-bonding solvents ranging from hexane to DMSO is the same for both the nitriles and matches with the earlier reported results.[1,30,40] A similar trend in aprotic solvents has been reported for carbonyl (C═O) vibrational probes where a red-shift in the C═O stretching frequency is also observed.[1,11,31−33]

3.1.2. Nitriles in H-Bonding Environment. When dissolved in a polar protic solvent like water, it has been reported that C═O shows a red-shift larger than that observed in DMSO.[11,31] The large red-shift of C═O in water can be rationalized by considering that a H-bond positions a large dipole near the IR probe due to the small van der Waals radius of hydrogen. It has also been recently shown that the C═O H-bonds are electrostatic and the solute−solvent interaction between C═O and water can be explained using VSE.[11,31,33] In contrary, when a nitrile (either PhCN or MeSCN) is dissolved in water, it can form a H-bond and $\bar{\nu}_{C\equiv N}$ is higher than that in DMSO (Figure S1). The blue shift in $\bar{\nu}_{C\equiv N}$ upon H-bonding contradicts the solute−solvent interaction to be a strictly dipole−dipole interaction based upon solvatochromic surveys and ab initio quantum mechanical calculations.[45,50,51,65−69] The H-bonding interactions in nitriles consist of nonelectrostatic contributions and hence the frequency shifts in H-bonded C≡N are not described by VSE.[40,47,68] To check the response of C≡N in a wide range of H-bonding solvation environments having intermediate polarities between DMSO and water, linear absorption experiments are performed in different aqueous binary mixtures of DMSO. Upon gradually increasing the water content in DMSO/water mixtures with 10% (v/v) increments, a monotonic increase in the blue-shift of $\bar{\nu}_{C\equiv N}$ is observed for both PhCN (Table 1 and Figure 1A) and MeSCN (Table 1 and Figure 1B)). Linear absorption experiments performed in DMF/water mixtures by changing the water content with 20% (v/v) increments show a similar blue-shifting trend of $\bar{\nu}_{C\equiv N}$ for both PhCN (Table 2 and Figure S2A) and MeSCN (Table 2 and Figure S2B). A similar set of linear IR experiments on C═O vibrational probes in DMSO/water mixture reports a monotonic red-shift in C═O frequencies from that in DMSO to water.[33]

Table 1. Nitrile Stretching Frequencies in DMSO−Water Mixtures

% of water in DMSO−water mixtures	C≡N stretching frequency/ cm^{-1}	
	PhCN	MeSCN
10	2227.7	2154.6
20	2228.1	2155.0
30	2228.7	2156.1
40	2230.0	2157.4
50	2230.9	2158.5
60	2232.3	2160.4
70	2233.3	2161.7
80	2234.0	2162.0
90	2234.7	2162.7
100	2235.3	2163.3

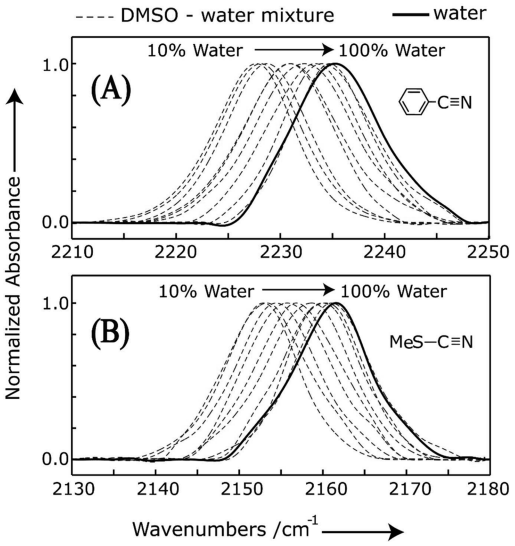

Figure 1. FTIR spectra of C≡N stretching band of (A) PhCN and (B) MeSCN in water and DMSO-water binary solvent mixtures at 10 mM concentrations. Nitrile stretching frequency gradually increases upon increasing the water content in DMSO/water mixtures by 10% (v/v).

Table 2. Nitrile Stretching Frequencies in DMF−Water Mixtures

% of water in DMF−water mixtures	C≡N stretching frequency/ cm^{-1}	
	PhCN	MeSCN
20	2228.8	2156.3
40	2230.7	2158.2
60	2233.0	2160.8
80	2234.3	2162.4
100	2235.3	2163.3

3.2. Electric Field in Non-H Bonding and H-Bonding Environment. In the solvatochromic IR experiments, the solutes are dissolved in different solvents of varying polarity and a microscopic and quantitative descriptor is required to relate the IR peak frequencies to noncovalent interactions. Dielectric constants and different polarity scales can characterize the solvent polarity based on an experimental observable in a quantitative manner; however, they cannot be related to (or calculated from) the microscopic arrangement of the molecules particularly for a highly heterogeneous medium like protein interiors. Though electric field can provide the microscopic picture, an appropriate model is required to estimate the field values. Onsager reaction field model, which has been used in the recent past, cannot account for specific chemical interactions.[1,31,32,70] In fact, the Onsager model predicts an almost constant electric field arising from polar solvation environments (dielectric constant > ∼40) irrespective of the ability of the solvent to participate in H-bonding with the solute (Figures S3A and S3B). On the contrary, average electric fields calculated from atomistic MD simulations can capture the microscopic details of the dielectric response of the solvent molecules and formation of H-bond with the vibrational probe, thereby accounting for both specific and nonspecific interactions. The instantaneous values of the electric field exerted on the probe may undergo huge fluctuations due to the inherent thermal motion of the solvent molecules leading to a

DOI: 10.1021/acs.jpcb.6b02732
J. Phys. Chem. B 2016, 120, 4034−4046

wide distribution of the field. We use the ensemble average electric field exerted on to the C≡N group, $F_{C\equiv N}$, by different solvation environments (including protic/aprotic solvents/mixtures) as the quantifier of the noncovalent interactions and local polarity experienced by the probe molecule. Due to presence of a permanent dipole moment on the C≡N bond, the effective electric field due to the polarization of the local solvent molecules will be along the dipole vector (C≡N bond) in an isotropic solvent medium. The electric fields calculated from MD simulations for neat solvents are tabulated in Table 3

Table 3. MD Estimated and Corrected Electric Fields Experienced by the Nitriles in Neat Solvents

solvents	MD estimated electric field/ (MV/cm)		corrected electric field /(MV/cm)[a]	
	PhCN	MeSCN	PhCN	MeSCN
hexanes	−0.08	−0.12	−0.03	−0.06
dibutylether	−7.57	−8.16	−2.73	−4.18
tetrahydrofuran (THF)	−14.85	−15.47	−5.36	−7.93
dimethylformamide (DMF)	−22.69	−23.55	−8.19	−12.08
dimethyl sulfoxide (DMSO)	−26.81	−27.89	−9.68	−14.30
water	−53.11	−49.59	−19.17	−25.43

[a]MD estimated fields are divided by 2.77 and 1.95 for PhCN and MeSCN, respectively, to get the corresponding corrected electric fields.

and the electric fields for solvent binary mixtures (DMSO/water and DMF/water mixtures) are tabulated in Tables 4 and

Table 4. MD Estimated and Corrected Electric Fields Experienced by the Nitriles in Different DMSO−Water Mixtures

% of water in DMSO−water mixtures	MD estimated electric field/ (MV/cm)		corrected electric field/(MV/cm)[a]	
	PhCN	MeSCN	PhCN	MeSCN
10	−27.98	−27.99	−10.10	−14.36
20	−30.77	−28.42	−11.11	−14.82
30	−32.59	−31.94	−11.77	−16.16
40	−37.20	−34.4	−13.43	−17.38
50	−41.84	−40.42	−15.10	−20.02
60	−43.77	−41.48	−15.80	−21.46
70	−46.16	−44.71	−16.66	−22.04
80	−48.97	−44.91	−17.68	−22.41
90	−50.92	−46.94	−18.38	−23.40
100	−53.11	−49.59	−19.17	−24.43

[a]MD estimated fields are divided by 2.77 and 1.95 for PhCN and MeSCN, respectively, to get the corresponding corrected electric fields.

5, respectively. The IR probe encounters the weakest solvation forces in nonpolar solvents and the calculated electric field is almost zero in hexanes for both PhCN and MeSCN. As a more polar environment would consist of solvent molecules with larger dipole moment, which can in turn exert a larger field, the average electric field ($F_{C\equiv N}$) increases as the polarity of the environment is increased from hexane to water (the negative sign in the electric field values implies a favorable electric field that lowers the solute's energy). For binary solvent mixtures, the increase in overall polarity as well as the H-bonding

Table 5. MD Estimated and Corrected Electric Fields Experienced by the Nitriles in Different DMF−Water Mixtures

% of water in DMF−water mixtures	MD estimated electric field/ (MV/cm)		corrected electric field/(MV/cm)[a]	
	PhCN	MeSCN	PhCN	MeSCN
20	−30.4	−29.66	−10.97	−15.21
40	−36.87	−35.71	−13.31	−18.31
60	−44.45	−40.87	−16.05	−20.96
80	−50.02	−44.91	−18.06	−23.03
100	−53.11	−49.59	−19.17	−24.43

[a]MD estimated fields are divided by 2.77 and 1.95 for PhCN and MeSCN, respectively, to get the corresponding corrected electric fields.

propensity with increasing water content leads to a larger average electric field. The peak position obtained from the IR experiment for an ensemble of solute molecules in solution can be related to the ensemble average electric field exerted on the IR probe.

3.3. Field-Frequency Correlation. *3.3.1. Nitriles in Non-H-Bonding Environment.* From VSE, the IR frequency shifts of PhCN and MeSCN depend on the electric field component ($F_{C\equiv N}$) along the respective C≡N bonds. $F_{C\equiv N}$ in aprotic solvents show an excellent linear correlation with the experimentally recorded $\bar{\nu}_{C\equiv N}$ with R^2 values of 0.99 for both PhCN (Figure 2A) and MeSCN (Figure 2B). The electrostatic (strictly dipole−dipole) interactions of the C≡N group with the aprotic solvent molecules lead to the linear dependence of the electric fields to C≡N frequencies through VSE. Similar correlations have been observed earlier both for aromatic and sulfur-based nitriles.[30,40,71] In the earlier studies, Onsager reaction field model was used to calculate the electric field exerted on the nitriles, where the cavity radius cubed was calculated by dividing the solute's formula weight by its density. As the interactions involving aprotic solvents are predominantly electrostatic, the slopes of the best-fit lines are theoretically equivalent to the respective Stark tuning rates, which can be independently measured for the nitrile group in both aromatic and sulfur based nitriles.[30,40] Excellent agreement had been observed in the earlier studies between the slopes (obtained using Onsager model) and the experimentally measured Stark tuning rates. However, Boxer and co-workers later used MD simulations for field calculations of C=O probes and reported that the use of the cavity volume instead of cavity radius in Onsager model would imply a mismatch between the Stark tuning rate and the slope.[31] In other words, the calculated electric field values were underestimated by a factor of $4\pi/3$, uniformly across all solvents.[30,40] In an another study Levinson et al. have illustrated that in the case of a molecule where the overall dipole moment is either zero (1,4 dicyano benzonitrile) or perpendicular to the nitrile bond (5-nitro-2-aminobenzonitrile), Onsager model fails to explain the solvatochromic behavior of nitrile even in non-H-bonded environments.[71] The solvatochromic responses of nitrile IR stretch in these cases exist due to the local dipole which orients solvent molecule around the C≡N bond and therefore the nitrile vibration depends on the polarity of the solvents. This further demonstrates the fact that Onsager model of field calculation lacks the microscopic details of the molecular interactions present between solutes and solvents in solution. On the

DOI: 10.1021/acs.jpcb.6b02732
J. Phys. Chem. B 2016, 120, 4034−4046

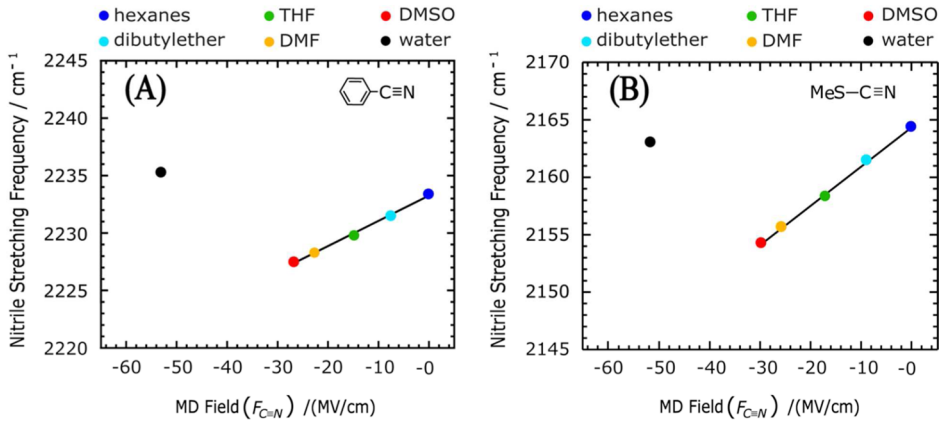

Figure 2. Field-frequency calibration for (A) PhCN and (B) MeSCN in non-H-bonding solvents. In purely electrostatic environment $\bar{\nu}_{C\equiv N}$ varies linearly with the electric field for both aromatic and sulfur based nitriles. The equations of the best-fit lines for (A) PhCN and (B) MeSCN are $\bar{\nu}_{C\equiv N}$ = 0.22 ($F_{C\equiv N}$) + 2233.3 (R^2 = 0.996) and $\bar{\nu}_{C\equiv N}$= 0.37 ($F_{C\equiv N}$) + 2164.3 (R^2 = 0.997) respectively. The field-frequency paired point (black circle) for the nitriles dissolved in water (H-bonded nitrile) falls off the best-fit lines. After correcting the electric field values to make the slopes of the best-fit lines the same as corresponding Stark tuning rates, the corrected equations for (A) PhCN and (B) MeSCN are $\bar{\nu}_{C\equiv N}$= 0.61 ($F_{C\equiv N}$) + 2233.3 (R^2 = 0.996) and $\bar{\nu}_{C\equiv N}$= 0.72 ($F_{C\equiv N}$) + 2164.3 (R^2 = 0.997), respectively.

contrary MD simulations can capture the full microscopic details of the solvation environment, and the electric field can be determined exactly at the midpoint of the bond connecting the diatomic IR probe by summing over the field due to all individual solvent molecules. The direction of the change in dipole moment (Stark tuning rate) is along the bond, and thus the determined electric fields provide meaningful information.

The slopes of the best fit lines from the MD simulations are 0.22 and 0.37 for Figure 2A,B, respectively. The reported values of the Stark tuning rate for aromatic and sulfur based nitriles are 0.61 cm^{-1}/(MV/cm) and 0.72 cm^{-1}/(MV/cm), respectively.[30,40] It is noteworthy that the solvatochromic slopes are smaller by factors of 2.77 and 1.95 from the corresponding experimentally measured Stark tuning rates. This difference arises from the local field effect and is consistent with the recently reported value of the local field correction factor, $f \approx 2$.[1] Henceforth in this manuscript, the estimated electric fields from MD simulations are reported after applying a correction factor of 2.77 and 1.95 for PhCN and MeSCN to make the slopes equal to the respective Stark tuning rates. The electric fields calculated from MD simulations for neat solvents, along with the corresponding corrected field values are tabulated in Table 3 and equations of the best fit lines of the two plots using the corrected fields are given in the captions of Figure 2A,B.

The field-frequency plot for non-H-bonded nitriles shows a similar linear trend as have been reported earlier, albeit using a semiempirical model, however the major difference lies in the choice of solvents. We have carefully excluded the aromatic and halogenated solvents while interrogating the electric field dependencies of the non-H-bonded nitrile frequencies to avoid any specific interactions like halogen bonding and π-stacking. Thus, the neat organic solvents only interact electrostatically with the nitrile group thereby shifting $\bar{\nu}_{C\equiv N}$ through VSE. This is well reflected in the R^2 values of ~0.99 in the linear fits shown in Figure 2 as compared to the R^2 values of ~0.7 as reported earlier.[40] As the slopes of these linear fits are compared with the experimentally reported $\Delta\vec{\mu}$ to obtain the correction factor, our results on non-H-bonded nitriles provide a better estimate of the electric field for a nitrile modified protein where the nitrile is buried in the hydrophobic pocket. A specific example using ribonuclease S (RNase S) has been discussed later.

3.3.2. Nitriles in H-Bonding Environments. Although nitriles show excellent field-frequency correlations in aprotic solvents, the correlations are violated when the nitriles are dissolved in a protic solvent (e.g., water). In the field-frequency plots (Figure 2A and 2B), the ($F_{C\equiv N}$, $\bar{\nu}_{C\equiv N}$) ordered point arising from neat water deviates from the best fit lines for both the nitriles. Earlier reports where Onsager reaction field model was used to estimate the nitrile electric fields, predict similar qualitative trend.[30,40] In spite of C═O H-bond interactions being electrostatic, a large deviation from the linear correlation was also observed for C═O using the semiempirical model as the Onsager model cannot account for the specific chemical interactions like H-bonding.[70] Using MD simulations, that include both H-bonded and non-H-bonded configurations, it was reported that C═O maintains the linear correlation for a protic solvent like water.[1,11,31,70] It has been demonstrated that if the solvation interactions are electrostatic, the linear dependence between field and frequency will be maintained (without any change of either the magnitude or the sign of the slope) irrespective of the H-bond donating capability of the solvent as long as $\Delta\vec{\mu}$ estimated from VSE is the same for the H-bonded and non-H-bonded IR probe.[31] The respective experimentally measured values of $\Delta\vec{\mu}$ have been reported to be unchanged in non-H-bonding and H-bonding environments for both nitrile and C═O IR probes.[31] Thus, if the H-bonding interactions in C≡N are electrostatic like C═O, the dotted lines in Figure S4A and Figure S4B would define the field-frequency correlation for H-bonded nitriles. However, any nonelectrostatic contribution to the noncovalent interaction cannot be described by VSE[40,47,50,51] and will result in a deviation from the dotted lines.

The values of $F_{C\equiv N}$ for PhCN and MeSCN in different binary aqueous mixtures of DMSO and DMF when plotted against the corresponding experimental frequencies show a distinct deviation from the respective dotted lines. The field-frequency point pairs obtained from two different aqueous binary mixtures that mimic the H-bonded solvation environment of the nitriles could be fitted to a new linear correlation with R^2 values of 0.99 (Figure 3A) and 0.97 (Figure 3B)

DOI: 10.1021/acs.jpcb.6b02732
J. Phys. Chem. B 2016, 120, 4034−4046

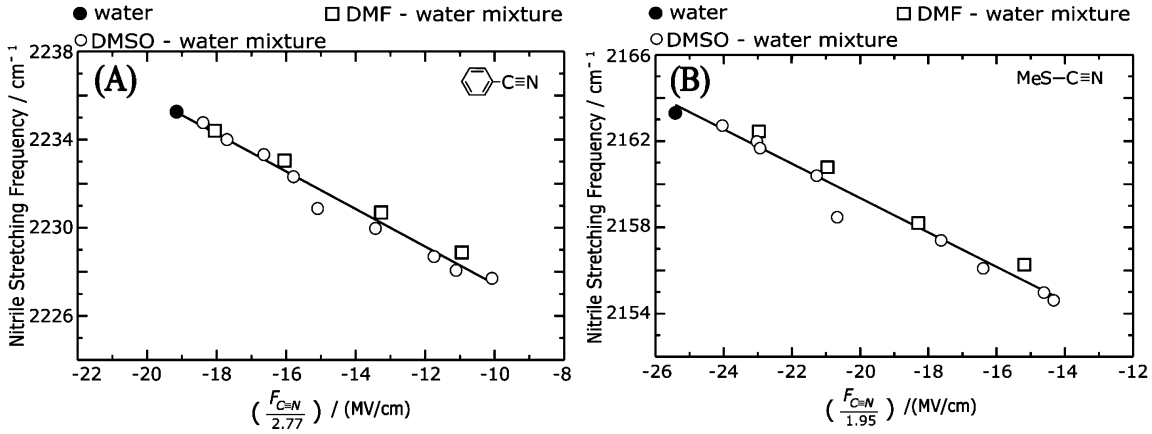

Figure 3. Field-frequency calibration for (A) PhCN and (B) MeSCN in of DMSO/water and DMF/water binary mixtures (H-bonding environments). A linear correlation between nitrile frequency and the electric field exerted by the H-bonding environments exists for both the aromatic and sulfur based nitriles. The equations of the best fit lines for (A) PhCN and (B) MeSCN are $\bar{\nu}_{C\equiv N}= -0.88\ (F_{C\equiv N}/2.77) + 2218.4$, ($R^2$ = 0.987) and $\bar{\nu}_{C\equiv N}= -0.80\ (F_{C\equiv N}/1.95) + 2143.4$, ($R^2$ = 0.97), respectively.

respectively. The slopes of the linear fits obtained for H-bonded C≡N, 0.88 and 0.80 for PhCN and MeSCN respectively, differ in magnitude from experimentally measured $\Delta\vec{\mu}$ and are also opposite in sign to that obtained in neat solvents. The deviation (from the dotted line of Figure S4) and the mismatch in magnitude and sign of the slopes portray a non-Stark behavior. Moreover, the dielectric constants of the nonaqueous component in the binary mixtures do not affect the field-frequency linearity of the H-bonded nitriles and our results indicate a possible existence of a general linear sensitivity of H-bonded $\bar{\nu}_{C\equiv N}$ to $F_{C\equiv N}$. This is further verified using THF–water binary mixtures (discussed later). The MD estimated and the corrected fields exerted on the C≡N group by various binary mixtures (DMSO/water and DMF/water) are given in Table 4 and Table 5.

3.4. Nitrile Bond Dipole in H-Bonding and Non-H-Bonding Environment. We have performed DFT calculations using B3LYP/6-31+G* basis set on PhCN to obtain a physical understanding of the overall blue-shift seen for H-bonded nitriles. Analysis of the partial charges on the C and the N atoms of C≡N show that the net charge difference (Δq) between C and N decreases (from that in an isolated molecule) upon H-bonding to a single water molecule. As Δq is proportional to the nitrile bond dipole ($\bar{\mu}_{C\equiv N}$), this leads to a decrease in $\bar{\mu}_{C\equiv N}$ upon H-bonding. On the other hand, if the specific interaction of H-bonding is ignored and the water solvation is treated using a polarization continuum model (PCM), $\bar{\mu}_{C\equiv N}$ increases. The interaction energy (U) can be defined as the nitrile bond dipole interacting with the electric field ($\vec{F}$) created by all the other molecules, i.e. $U = -\bar{\mu}_{C\equiv N}\cdot\vec{F}$. For an aqueous binary mixture, the ensemble average field exerted on C≡N increases with increasing water content. For any $\vec{F}$ (corresponding to a particular v/v of binary mixture), two competing processes shift $\bar{\nu}_{C\equiv N}$, namely a red shift (decrease in U) from the overall increase in polarity of the medium (i.e., VSE) and a blue shift (increase in U) from the specific H-bonding interaction. We believe that the extent of blue shift from H-bonding being larger than the red-shift from VSE creates an overall blue shift in the experimental values of $\bar{\nu}_{C\equiv N}$ from that in the neat solvent. We have also performed similar calculations on acetophenone. For C═O, $\bar{\mu}_{C=O}$ increases with increase in polarity of the medium as well as upon H-bonding. Thus, there are no competing spectral shifts in C═O and an overall red-shift has been observed in H-bonded C═O. The charges on the different atoms of the diatomic IR probes are listed in Table S1 of the Supporting Information. Detailed quantum chemical calculations, beyond the scope of this paper, are required to get a quantitative understanding of the field-frequency correlation of H-bonded nitrile.

The preliminary calculations reported here provides an understanding based on the change of the bond dipole, but cannot describe the linear dependence between $\bar{\nu}_{C\equiv N}$ and $F_{C\equiv N}$ in H-bonding environments. To describe the linear field-frequency correlation in nitriles, we have also included a qualitative empirical model in the Supporting Information where we consider $\bar{\nu}_{C\equiv N}$ to be the weighted average of the average frequencies corresponding to the overlapping H-bonded and non-H-bonded populations. This model, as it turns out, can also describe the opposite trend that has been reported for C═O. For nitriles in any binary solvent mixture, the change in $\bar{\nu}_{C\equiv N}$ from that in the neat organic solvent is a combination of electrostatic red-shift and the nonelectrostatic blue-shift from H-bonding. Our empirical model assumes $\Delta\bar{\nu}$, the frequency shift between H-bonded and non-H-bonded C≡N, is positive (as seen for DMSO and DMF). In other words, upon addition of water to any pure solvent, the nonelectrostatic contribution to $\bar{\nu}_{C\equiv N}$ is greater than the electrostatic contribution from VSE, thereby causing an overall blue-shift in$\bar{\nu}_{C\equiv N}$. However, our simple model is not expected to work in cases where the red shift from VSE is larger than the blue-shift from H-bonding. Quantitatively, the error will be more for a larger polarity difference between the nonaqueous solvent and water where only a very small fraction of the solute is H-bonded.

3.5. Nitrile Line Shape Analysis. The nitrile line width depends on the ultrafast picosecond dynamics of its local environment that arises primarily from the solvent dipolar fluctuations in the solvatochromic experiments. The electric field distribution on the nitrile probe for any solvent/binary mixture also captures the fluctuations of the surrounding solvent molecules. However, the line width of an IR band is a dynamic quantity that depends on correlations in the frequency

DOI: 10.1021/acs.jpcb.6b02732
J. Phys. Chem. B 2016, 120, 4034–4046

fluctuations (including motional narrowing) rather than just the distribution of fields sampled. Moreover, any change in the H-bond making and breaking dynamics of nitriles in aqueous binary mixtures would be reflected only in the experimental spectra. We have a few important observations from the line shape analysis of the IR absorption spectra and the field distributions. We observe (Figure S5) that a solvent which exerts larger electric fields will also produce a more heterogeneous field distribution of electric fields (resulting in a broader peak). Moreover, for the neat solvents, a larger fwhm of the IR spectrum corresponds to an increased standard deviation of the field distribution. This correlation become more complex for the aqueous binary mixtures. When, C≡N band line width of PhCN is plotted (Figure S6) against the standard deviation of the field distribution for each solvent/solvent mixture, the strength of the linear correlation is only moderate (R^2 = 0.70), indicating that standard deviation is not sufficient to explain all the variation in experimental fwhm, and suggesting that the field correlations are not uniform across the solvent series. 2D-IR results have shown the solute hydrogen bond dynamics becomes slower by a factor of 5 for 50% DMSO/water (v/v) as compared to that in neat water.[72] However, the solvent fluctuation is faster in water as compared with binary mixtures. Thus, a larger field distribution in neat water can be motionally narrowed and the relatively smaller field distribution in a binary mixture might have a broader IR bandwidth due to the slower exchange rate. To get accurate information on the fluctuation and hydrogen bond exchange time scales, time-resolved IR experiments (2D-IR) need to be done, which lie outside the scope of this work.

3.6. Significance of the Field-Frequency Correlation in H-Bonded Nitriles. The electric fields, as shown in cases of PhCN and MeSCN, can be calculated directly from MD simulations. However, apart from the approximations involved in the force field, the determination of the electric field for large biological macromolecules like peptides and proteins is itself computationally expensive. To date, the linear correlation between $\bar{\nu}_{C\equiv N}$ and $F_{C\equiv N}$ for nonspecific interactions of the nitrile group has been known from VSE.[30,40] This has permitted the quantitative estimation of the noncovalent interactions in nitriles and nitrile modified biomolecules directly from IR absorption experiments, as long as the nitrile group is not H-bonded. The nonelectrostatic nature associated with H-bonded nitrile could not be described by VSE, which severely limited the use of a nitrile to probe specific noncovalent interactions. As specific interactions like H-bonding with side chains, bound ligands and neighboring water molecules are prevalent in biomolecules, the nitrile chemical group, in spite of having several advantages as a biomolecular site-specific spectroscopic probe, could not be extensively used to quantify noncovalent interactions where the nitrile is H-bonded.

We have shown that a linear correlation between field and frequency exists for small molecule nitriles in aqueous mixtures. However, there is no particular reason that any of these environmental factors in aqueous binary mixtures should particularly resemble the environment around the side chain of an artificial amino acid in a protein. In a heterogeneous biomolecular system, the nitrile surrounding consists of many atoms which are either part of the molecular architecture of the protein or the surrounding solvent molecules. The electrostatic field estimated at the nitrile moiety depends on the distances of all the other atoms in the system from the nitrile probe as well as the residual partial charges on each atom. Thus, aqueous binary mixtures serve the purpose of reporting the electric field values between the most polar aprotic solvent and water where the electric field provides microscopic insight independent of the identity of the surrounding atoms. Moreover, experimentally accessible different aqueous binary mixtures can provide the average $\bar{\nu}_{C\equiv N}$ within a distribution of conformations where at least some fraction is H-bonded. Thus, the binary solvent mixtures provide us with an opportunity to correlate the experimentally obtained H-bonded $\bar{\nu}_{C\equiv N}$ with the corresponding $F_{C\equiv N}$ as obtained from simulations. If a single correlation exists for multiple aqueous binary mixtures, the average experimental frequency observed in biomolecules can predict the associated electric field. In other words, the linear dependence in H-bonding environments can be generalized to other systems and the best-fit line obtained for binary mixtures should act as a calibration curve to predict electric fields in complex biomolecular systems directly from IR measurements. Thus, the linear correlation reported here for H-bonded nitriles, coupled with the practical utility of the nitrile IR probe, opens up a new and direct experimental avenue to report on the specific noncovalent interactions in biomolecules.

3.7. Validation of the Field-Frequency Correlation in H-Bonded Nitriles. To test the generality of the linear dependence of the nitrile IR frequencies to the electric fields in H-bonded environments, we have investigated its robustness for H-bonded aromatic and sulfur based aliphatic nitriles in a wide range of nitrile containing molecules of varying size, compactness and solvation environments. Calibration curves have been constructed for the nitriles from the respective field-frequency correlations (best fit lines in Figure 3) using aqueous binary mixtures.

3.7.1. Small Molecule Model Nitriles. For nitriles in DMSO (DMF)/water mixtures, where both C≡N and DMSO (DMF) are H-bond acceptors, nitriles can only form H-bonds with the water molecules present in the binary solvent mixture. On the contrary, in the presence of a denaturant like urea in aqueous environment, C≡N can form H-bonds either with water or urea molecules. It has been suggested that studying the effect of denaturants on the $\bar{\nu}_{C\equiv N}$ in aqueous solutions of model nitriles can provide insights about the mechanism of protein denaturation.[73] We have performed IR absorption experiments to obtain nitrile IR frequencies for PhCN and MeSCN in aqueous urea (5M) solution. The peak frequencies of the C≡N group of both the sulfur based and aromatic nitriles in 5 M urea shift to a lower value compared to that in aqueous solution. A similar red-shift of the C≡N stretching frequency in the presence of urea has been previously reported by Gai and co-workers for acetonitrile.[73] From the respective calibration curves (Figure 3A,B), we have predicted the electric fields, which agree with the independently estimated fields from MD simulations. This agreement validates the field-frequency calibration of H-bonded nitriles for small molecules in a complex solvation environment. The predicted and estimated electric fields are listed in Table 4.

3.7.2. Nitrile Modified Amino Acid. To investigate whether H-bonded $\bar{\nu}_{C\equiv N}$can quantitatively predict the electric fields in biomolecules, we have tested our calibration curve on an amino acid, since they serve as the building block of any peptide or protein. We have synthesized a modified cysteine (Compound **3** of the Supporting Information) by incorporating a PhCN unit into the amino acid. The details of the synthesis of **3** are

DOI: 10.1021/acs.jpcb.6b02732
J. Phys. Chem. B 2016, 120, 4034−4046

Table 6. Comparison of the Predicted Electric Fields with the MD Estimated Values in Model Nitriles in Complex Solvation Environment, in a Nitrile Modified Amino Acid and in a Nitrile Modified Protein

samples	nitrile stretching frequency/(cm^{-1})	figure used[a]	corrected electric field on nitrile /(MV/cm) predicted	corrected electric field on nitrile /(MV/cm) estimated from MD	prediction error /(MV/cm)[b]
PhCN in aqueous urea (5 M) solution	2234.4	Figure 3A	−18.18	−19.35	1.17
MeSCN in aqueous urea (5 M) solution	2162.0	Figure 3B	−23.38	−26.33	3.04
nitrile modified amino acid (compound 3)	2236.7	Figure 3A	−20.80	−21.07	0.27
nitrile modified protein (compound 7)	2234.2	Figure 4	−17.96	−19.08	1.12
[p-CN-Phe]RNase S	2231	Figure 2A	−3.77	−2.82	0.95

[a]Iindicates the best-fit line of the figure used to predict the electric field. [b]Prediction error is the absolute value of difference between the predicted and the estimated electric fields.

Table 7. Comparison of the Experimental and Predicted IR Frequencies in Nitrile Modified Peptides

peptides	mutant position	corrected electric field on nitrile/(MV/cm)	figure used[a]	nitrile stretching frequency /(cm^{-1}) predicted	nitrile stretching frequency /(cm^{-1}) experimental	prediction error[b]/(cm^{-1})
Mastoparan X	6	−18.48	Figure 3A	2234.7	2234.9	0.2
	9	−19.32		2235.4	2235.1	0.3
	10	−19.35		2235.4	2235.2	0.2
CM15	4	−23.19	Figure 3B	2161.9	2161.6	0.3
	10	−22.91		2161.6	2161.2	0.4

[a]Indicates the best-fit line of the figure used to predict the IR frequency. [b]Prediction error is the absolute value of difference between the predicted and the estimated frequencies.

given in the Supporting Information. The synthesis of **3**, using a slightly different protocol, has been reported earlier to demonstrate that the cysteine alkylation can serve as an effective alternative to introduce aromatic nitriles into peptides and proteins.[74] The experimental $\bar{\nu}_{C\equiv N}$ (2236.7 cm^{-1}) of the modified amino acid corresponds to a field value of 20.80 MV/cm as predicted by extrapolating the best fit line. The MD estimated field for **3** shows an excellent agreement and is within 0.27 MV/cm of the predicted field (Table 6). Here $\bar{\nu}_{C\equiv N}$ is 1.4 cm^{-1} higher than that of PhCN in neat water and thereby the value of the electric field is larger than the field experienced by the model nitrile (PhCN) in aqueous environments. This result underpins the extendibility of the field-frequency correlation to higher absolute field values than that obtained for H-bonded model nitrile in water. The predicted and estimated electric fields on the nitrile group of the modified cysteine are listed in Table 6.

3.7.3. Nitrile Modified Peptides. Further to validate the robustness of the calibration curves in peptides, multiple mutants of two peptides, one with an aromatic nitrile and the other with an sulfur based nitrile are surveyed. For each peptide we have performed MD simulations to estimate $F_{C\equiv N}$. The corresponding nitrile IR frequencies predicted using the calibration curves are compared with the earlier reported experimental results.[53,54] The C≡N group in the respective peptides has been proposed to be solvent (water) exposed in each of the mutants, thereby accepting H-bond from the solvent molecules.[53,54]

We have estimated the electric fields experienced by the C≡N probe along the nitrile bond for nitrile-modified mutants of Mastoparan X (Mp-X) and the antimicrobial peptide CM15. For the aromatic nitrile modified Mp-X, MD field calculations have been done for three mutants in water, where p-CN-Phe is introduced at positions 6, 9, and 10 of the peptide sequence in each mutant, respectively. The predicted nitrile stretching frequencies along with the experimental values are listed in Table 7. In an earlier report, Gai and co-workers reported the nitrile stretching frequencies for these three mutants and mentioned that the p-CN-Phe residues to be fully hydrated (i.e., C≡N is H-bonded) when dissolved in water.[53] Our predicted frequencies for the MP-X mutants match with the experimental frequencies within 0.3 cm^{-1} (Table 7). Further, we have performed MD simulations to find out $F_{C\equiv N}$ for two of the mutants of CM15 peptide (Cys-SCN introduced at either positions 4 and 10) using the same protocol used for Mp-X mutants. Our predicted frequencies are in excellent agreement with the experimental frequencies as recorded by Londergan and co-workers.[54] These results confirm that the field-frequency correlation is not only applicable to small nitrile containing molecules, but also for biologically relevant peptides. These peptides are inherently structurally disordered, and can exist in a wide distribution of conformations in aqueous solutions. The excellent agreement of the predicted and experimental $\bar{\nu}_{C\equiv N}$ suggests that site-specific noncovalent interactions can be quantitatively estimated in nitrile modified peptides in an inhomogeneously broadened aqueous environment.

3.7.4. Nitriles in THF/Water Mixture. DMSO/water mixture is one of the aqueous binary mixtures used to calibrate the sensitivity of $\bar{\nu}_{C\equiv N}$ with the corresponding $F_{C\equiv N}$. As DMSO is strong dipolar, it can be argued that it is not relevant to the kinds of local fields that might be possible in many biomolecular systems. On the other hand, THF, due to its low dielectric constant and reduced polarity as compared to water, can be regarded as a reasonable bulk model for the protein interior or an environment of similar hydrophobicity. We have used THF/water binary mixtures to check the validity of the field-frequency calibration of hydrogen bonded nitrile for both PhCN and MeSCN. The electric fields obtained for increasing concentrations of THF in the binary mixtures from the IR frequencies (Table S3) and the corresponding calibration curve show a good agreement with that predicted

DOI: 10.1021/acs.jpcb.6b02732
J. Phys. Chem. B 2016, 120, 4034−4046

Table 8. Comparison of the Predicted Electric Fields with the MD Estimated Values in Model Nitriles in THF−Water Binary Mixtures

	nitrile IR stretch/cm^{-1}		predicted field/(MV/cm)		corrected MD field field/(MV/cm)		prediction error[a]/(MV/cm)	
% of water in THF−water mixtures	PhCN	MeSCN	PhCN	MeSCN	PhCN	MeSCN	PhCN	MeSCN
40	2229.8	2156.8	−12.95	−16.75	−11.76	−14.90	1.19	1.85
60	2231.6	2160.9	−14.89	−21.88	−13.54	−18.04	1.35	3.84
80	2234.8	2161.3	−18.52	−22.38	−17.51	−23.27	1.01	0.89

[a]Prediction error is the absolute value of difference between the predicted and the estimated electric fields.

independently from MD simulations (Table 8). Most of the peptides/protein used as test molecules to check the generality of the solvatochromic calibration for H-bonded nitriles have the nitrile group exposed to water. On the other hand, 60% and 40% THF/water solutions validate the low-frequency regions of the calibration curve for H-bonded C≡N. As THF can be considered as a reasonable model to mimic protein hydrophobic environment, THF/water results demonstrates that electric field can be estimated for H-bonded nitriles, in cases where the extent of hydration is less and the nitrile is H-bonded to an amino acid side chain.

3.7.5. Nitrile Modified Protein. In biological macromolecules like proteins and enzymes, theoretical determination of the electric field is computationally expensive. It would be extremely helpful to get the quantitative information on local electric field exerted on the nitrile modified proteins in H-bonding environments from simple IR experiments using the field-frequency calibration. Linear IR absorption experiments are performed to obtain $\bar{\nu}_{C\equiv N}$ of nitrile modified protein (compound **7** of Supporting Information) where PhCN has been attached with the Cys-34 unit of the bovine serum albumin (BSA) through a linker (compound **6** of the Supporting Information). The C≡N stretching frequencies of **6** are independently measured in multiple solvents and compared with the nitrile stretch of PhCN (as shown in Table S1). C≡N stretching frequencies are found be to within 0.1 cm^{-1} for the linker and PhCN. This result suggests that PhCN can be used as a model nitrile for the linker and the linker conjugated protein.

Synthesis of **6** and **7** have been discussed in the Supporting Information. The bioconjugation of the aromatic nitrile group with Cys-34 (only free cysteine in BSA) is achieved under nonreductive conditions to keep the disulfide bonds between the other Cys residues unperturbed. From tryptic digestion of **7** it has been confirmed that modification occurred only at the Cys-34 residue of BSA. The nitrile stretching frequency of **7** is recorded in aqueous buffer and the electric field experienced by the nitrile group is predicted to be −17.96 MV/cm from the field-frequency correlation plot (Figure 4A,B) which is in good agreement with the electric field value of −19.08 MV/cm, determined independently using MD simulations (Figure 4C). The experimental IR absorption spectrum of the nitrile modified protein in shown in Figure S8. This observation firmly suggests that our model is appropriate for predicting electric fields experienced by H-bonded nitrile groups in biological macromolecules. The protein is structurally ordered as compared with the earlier mentioned disordered peptides. The ability to estimate specific noncovalent interactions in both the disordered and ordered biomolecules illustrates the generality of the field-frequency correlation for H-bonded nitriles.

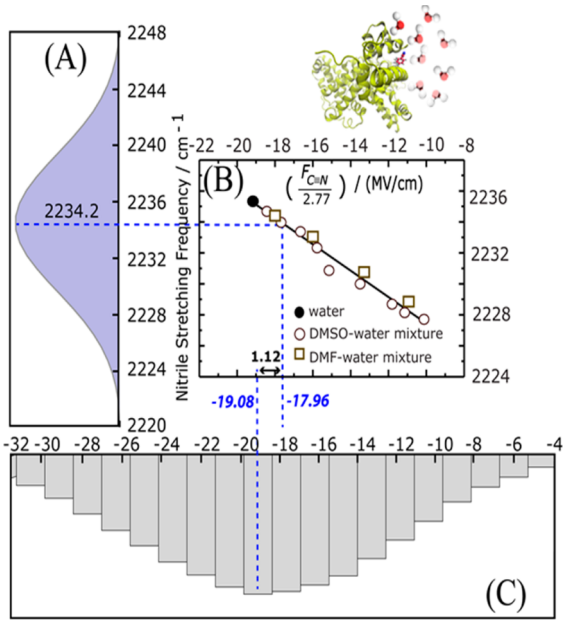

Figure 4. Field-frequency correlation acts a calibration curve to predict the electric field experienced by the nitrile modified bovine serum albumin (compound **7**). (A) The nitrile stretch region of the FTIR spectrum of compound **7**, fitted to a Gaussian profile. (B) The field-frequency correlation plot from Figure 2A to predict $F_{C\equiv N}$ of the nitrile modified protein from the C≡N peak frequency of compound **7**. (C) Histograms of the estimated electric fields from MD simulations (divided by the 2.77, the scaling factor for PhCN) of compound **7**. The predicted field value from the calibration curve, −17.96 MV/cm, differs from the estimated field value, −19.08 MV/cm, by 1.12 MV/cm.

3.8. Validation of the Field-Frequency Correlation in Buried Nitrile. We have also considered a case where nitrile is buried in a protein ribonuclease S (RNase S) which is a limited proteolysis product, generated when a protease enzyme, subtilisin acts on RNase A. From the crystal structure of nitrile modified RNase S ([p-CN-Phe]RNase S) it has been seen that the nitrile group remains buried in a hydrophobic region which is close to active site of the protein and no hydrogen bond donating group is present near the nitrile group.[35] In an earlier study Boxer and co-workers have reported $\bar{\nu}_{C\equiv N}$ of [p-CN-Phe]RNase S and mentioned that PhCN can be used as a model nitrile for the nitrile variant of the protein.[30] Using field-frequency correlations in Figure 2A as the calibration curve, we have predicted the electric field on the nitrile of ([p-CN-Phe]RNase S. The predicted $F_{C\equiv N}$ shows an excellent agreement (within 0.95 MV/cm) with the MD estimated electric field (Table 6). Boxer and co-workers have also estimated the $F_{C\equiv N}$ of [p-CN-Phe]RNase S from field-frequency correlation constructed using the Onsager model.

DOI: 10.1021/acs.jpcb.6b02732
J. Phys. Chem. B 2016, 120, 4034−4046

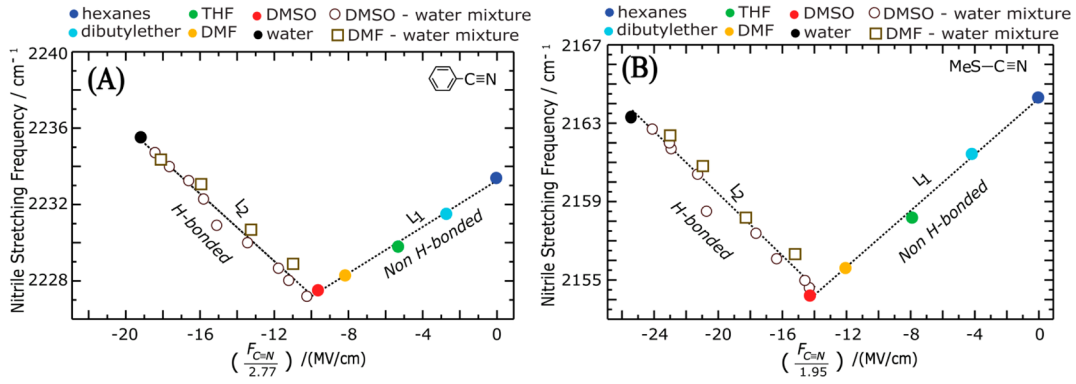

Figure 5. "V-shaped" combined field-frequency correlation can act as a calibration curve for (A) PhCN and (B) MeSCN in H-bonding and non-H-bonding environments. Depending upon the specificity of the noncovalent interactions, L_1 or L_2 can be chosen as the calibration curve to predict electric field from experimental IR frequency.

However, it was later mentioned by Boxer and co-workers that the Onsager model overestimates the electric field.[31] The current agreements shown in this work for RNase S and BSA show that $F_{C\equiv N}$ can be predicted both for H-bonded and non-H bonded nitriles in proteins using calibration curves constructed from IR experiments and MD simulations on model nitrile compounds.

3.9. Prediction of Electric Fields without a Priori Knowledge about H-Bonding. We have shown and validated a direct correlation between nitrile stretching frequency and the electric field experienced by the nitrile group in H-bonding environments (Figure 3). Combining Figure 3 with the field-frequency correlation for nitrile in non-H-bonded environments (Figure 2) provides an interesting V-shaped plot (Figure 5A and Figure 5B) in which line L_1 represents the behavior of nitriles in non-H-bonded environments and line L_2 represents the same in H-bonded environments. As can be seen from Figure 5, the ensemble average value of $\bar{\nu}_{C\equiv N}$ obtained from IR experiments can correspond to two values of the electric field, depending on the specificity of the noncovalent interaction. To predict the site-specific electric field experienced by a nitrile modified biomolecule directly from IR absorption experiments, the knowledge of the H-bonding status of the nitrile is required, which can be confirmed either from IR-NMR correlations or from the structural information on the nitrile containing compounds.[30,40] Once the H-bonding status is known, the corresponding best-fit line (either L_1 or L_2) can be utilized to quantify the noncovalent interactions. This way, electric field approach can be generalized to quantify any noncovalent interaction of nitrile containing biomolecules or ligands, specific or nonspecific.

4. CONCLUDING REMARKS

We have demonstrated and validated a linear field-frequency correlation for specific chemical interactions like H-bonding in nitriles in a range of molecules of different size and compactness. Such a correlation has never been reported until date and our current findings can be useful to estimate electric fields experienced by the H-bonded nitriles and thereby increase the utility of the nitrile vibrational probe. Further, these results allow us to describe the H-bonded and non-H-bonded environments of a nitrile vibrational probe in a consistent manner through average electric fields arising from the environment, which has been suggested as one of the most important microscopic descriptors of noncovalent interactions. The field-frequency correlation obtained for the nitriles illustrates that nitrile vibrational probes, like carbonyls, can also be benchmarked against reference data, providing a consistent way out to interpret nitrile frequencies in complex molecular systems, in both H-bonding and non-H-bonding environments. These results might provide a valuable quantitative understanding of the noncovalent interactions and their roles toward molecular recognition and molecular self-assembly in either nitrile containing drugs or nitrile modified proteins in any chemical environment.

■ ASSOCIATED CONTENT

Supporting Information

The Supporting Information is available free of charge on the ACS Publications website at DOI: 10.1021/acs.jpcb.6b02732.

FTIR spectra of the model nitriles and the FTIR spectra of the nitrile modified BSA in buffer solution. Synthetic details of the nitrile modified amino acid, nitrile modified linker and the bioconjugation of the linker to the protein. Supporting Tables and Figures as mentioned in the main text. Empirical model. (PDF)

■ AUTHOR INFORMATION

Corresponding Authors

*E-mail: s.bagchi@ncl.res.in. Phone: + 91-20-25903048. Fax: + 91-20-25902636.

*E-mail: s.chakrabarty@ncl.res.in. Phone: + 91-20-25903053. Fax: + 91-20-25902636.

Notes

The authors declare no competing financial interest.

■ ACKNOWLEDGMENTS

This work has been financially supported by CSIR-NCL start-up grants (MLP028126 and MLP027526). S.C. and S.B. thank the Department of Science and Technology (DST), India for the Ramanujan Fellowship. S.C. thanks CSIR, India for funding from XIIth five year plan on Multiscale Modelling (CSC0129). P.D. thanks Department of Science and Technology (DST), India for the INSPIRE Fellowship. We thank Dr. Sayam Sen Gupta (CSIR-NCL), Bhawana Pandey and Sushma Kumari for valuable suggestions regarding nitrile bioconjugation to the protein. We thank Dr. Mahesh Kulkarni and Garikapati Vannuruswamy for their help regarding trypsin digestion.

DOI: 10.1021/acs.jpcb.6b02732
J. Phys. Chem. B 2016, 120, 4034−4046

REFERENCES

(1) Fried, S. D.; Boxer, S. G. Measuring Electric Fields and Noncovalent Interactions Using the Vibrational Stark Effect. *Acc. Chem. Res.* **2015**, *48*, 998−1006.

(2) Lehn, J. M. Supramolecular Chemistry - Scope and Perspectives Molecules, Supermolecules, and Molecular Devices. *Angew. Chem., Int. Ed. Engl.* **1988**, *27*, 89−112.

(3) Warshel, A.; Sharma, P. K.; Kato, M.; Xiang, Y.; Liu, H.; Olsson, M. H. M. Electrostatic Basis for Enzyme Catalysis. *Chem. Rev.* **2006**, *106*, 3210−3235.

(4) Warshel, A.; Aqvist, J. Electrostatic Energy and Macromolecular Function. *Annu. Rev. Biophys. Biophys. Chem.* **1991**, *20*, 267−298.

(5) Kamerlin, S. C. L.; Sharma, P. K.; Chu, Z. T.; Warshel, A. Ketosteroid Isomerase Provides Further Support for the Idea That Enzymes Work by Electrostatic Preorganization. *Proc. Natl. Acad. Sci. U. S. A.* **2010**, *107*, 4075−4080.

(6) Adamczyk, A. J.; Cao, J.; Kamerlin, S. C. L.; Warshel, A. Catalysis by Dihydrofolate Reductase and Other Enzymes Arises from Electrostatic Preorganization, Not Conformational Motions. *Proc. Natl. Acad. Sci. U. S. A.* **2011**, *108*, 14115−14120.

(7) Jha, S. K.; Ji, M.; Gaffney, K. J.; Boxer, S. G. Direct Measurement of the Protein Response to an Electrostatic Perturbation That Mimics the Catalytic Cycle in Ketosteroid Isomerase. *Proc. Natl. Acad. Sci. U. S. A.* **2011**, *108*, 16612−16617.

(8) Strajbl, M.; Shurki, A.; Kato, M.; Warshel, A. Apparent Nac Effect in Chorismate Mutase Reflects Electrostatic Transition State Stabilization. *J. Am. Chem. Soc.* **2003**, *125*, 10228−10237.

(9) Wu, N.; Mo, Y. R.; Gao, J. L.; Pai, E. F. Electrostatic Stress in Catalysis: Structure and Mechanism of the Enzyme Orotidine Monophosphate Decarboxylase. *Proc. Natl. Acad. Sci. U. S. A.* **2000**, *97*, 2017−2022.

(10) Honig, B.; Nicholls, A. Classical Electrostatics in Biology and Chemistry. *Science* **1995**, *268*, 1144−1149.

(11) Fried, S. D.; Bagchi, S.; Boxer, S. G. Extreme Electric Fields Power Catalysis in the Active Site of Ketosteroid Isomerase. *Science* **2014**, *346*, 1510−1514.

(12) Camilloni, C.; Sahakyan, A. B.; Holliday, M. J.; Isern, N. G.; Zhang, F.; Eisenmesser, E. Z.; Vendruscolo, M. Cyclophilin a Catalyzes Proline Isomerization by an Electrostatic Handle Mechanism. *Proc. Natl. Acad. Sci. U. S. A.* **2014**, *111*, 10203−10208.

(13) Liu, C. T.; Layfield, J. P.; Stewart, R. J., III; French, J. B.; Hanoian, P.; Asbury, J. B.; Hammes-Schiffer, S.; Benkovic, S. J. Probing the Electrostatics of Active Site Microenvironments Along the Catalytic Cycle for Escherichia Coli Dihydrofolate Reductase. *J. Am. Chem. Soc.* **2014**, *136*, 10349−10360.

(14) Kamerlin, S. C. L.; Warshel, A. At the Dawn of the 21st Century: Is Dynamics the Missing Link for Understanding Enzyme Catalysis? *Proteins: Struct., Funct., Genet.* **2010**, *78*, 1339−1375.

(15) Park, E. S.; Andrews, S. S.; Hu, R. B.; Boxer, S. G. Vibrational Stark Spectroscopy in Proteins: A Probe and Calibration for Electrostatic Fields. *J. Phys. Chem. B* **1999**, *103*, 9813−9817.

(16) Suydam, I. T.; Snow, C. D.; Pande, V. S.; Boxer, S. G. Electric Fields at the Active Site of an Enzyme: Direct Comparison of Experiment with Theory. *Science* **2006**, *313*, 200−204.

(17) Thielges, M. C.; Case, D. A.; Romesberg, F. E. Carbon-Deuterium Bonds as Probes of Dihydrofolate Reductase. *J. Am. Chem. Soc.* **2008**, *130*, 6597−6603.

(18) Ye, S.; Huber, T.; Vogel, R.; Sakmar, T. P. Ftir Analysis of Gpcr Activation Using Azido Probes. *Nat. Chem. Biol.* **2009**, *5*, 397−399.

(19) Li, T. S.; Quillin, M. L.; Phillips, G. N.; Olson, J. S. Structural Determinants of the Stretching Frequency of CO Bound to Myoglobin. *Biochemistry* **1994**, *33*, 1433−1446.

(20) Taskent-Sezgin, H.; Chung, J.; Banerjee, P. S.; Nagarajan, S.; Dyer, R. B.; Carrico, I.; Raleigh, D. P. Azidohomoalanine: A Conformationally Sensitive IR Probe of Protein Folding, Protein Structure, and Electrostatics. *Angew. Chem., Int. Ed.* **2010**, *49*, 7473−7475.

(21) Hu, W.; Webb, L. J. Direct Measurement of the Membrane Dipole Field in Bicelles Using Vibrational Stark Effect Spectroscopy. *J. Phys. Chem. Lett.* **2011**, *2*, 1925−1930.

(22) Shrestha, R.; Cardenas, A. E.; Elber, R.; Webb, L. J. Measurement of the Membrane Dipole Electric Field in DMPC Vesicles Using Vibrational Shifts of P-Cyanophenylalanine and Molecular Dynamics Simulations. *J. Phys. Chem. B* **2015**, *119*, 2869−2876.

(23) Cho, M. Vibrational Solvatochromism and Electrochromism: Coarse-Grained Models and Their Relationships. *J. Chem. Phys.* **2009**, *130*, 094505.

(24) Bublitz, G. U.; Boxer, S. G. Stark Spectroscopy: Applications in Chemistry, Biology, and Materials Science. *Annu. Rev. Phys. Chem.* **1997**, *48*, 213−242.

(25) Boxer, S. G. Stark Realities. *J. Phys. Chem. B* **2009**, *113*, 2972−2983.

(26) Ma, J.; Pazos, I. M.; Zhang, W.; Culik, R. M.; Gai, F. Site-Specific Infrared Probes of Proteins. *Annu. Rev. Phys. Chem.* **2015**, *66*, 357−377.

(27) van Wilderen, L. J. G. W.; Kern-Michler, D.; Mueller-Werkmeister, H. M.; Bredenbeck, J. Vibrational Dynamics and Solvatochromism of the Label SCN in Various Solvents and Hemoglobin by Time Dependent IR and 2D-IR Spectroscopy. *Phys. Chem. Chem. Phys.* **2014**, *16*, 19643−19653.

(28) Park, E. S.; Thomas, M. R.; Boxer, S. G. Vibrational Stark Spectroscopy of No Bound to Heme: Effects of Protein Electrostatic Fields on the No Stretch Frequency. *J. Am. Chem. Soc.* **2000**, *122*, 12297−12303.

(29) Andrews, S. S.; Boxer, S. G. Vibrational Stark Effects of Nitriles I. Methods and Experimental Results. *J. Phys. Chem. A* **2000**, *104*, 11853−11863.

(30) Bagchi, S.; Fried, S. D.; Boxer, S. G. A Solvatochromic Model Calibrates Nitriles' Vibrational Frequencies to Electrostatic Fields. *J. Am. Chem. Soc.* **2012**, *134*, 10373−10376.

(31) Fried, S. D.; Bagchi, S.; Boxer, S. G. Measuring Electrostatic Fields in Both Hydrogen-Bonding and Non-Hydrogen-Bonding Environments Using Carbonyl Vibrational Probes. *J. Am. Chem. Soc.* **2013**, *135*, 11181−11192.

(32) Pazos, I. M.; Ghosh, A.; Tucker, M. J.; Gai, F. Ester Carbonyl Vibration as a Sensitive Probe of Protein Local Electric Field. *Angew. Chem., Int. Ed.* **2014**, *53*, 6080−6084.

(33) Kashid, S. M.; Bagchi, S. Experimental Determination of the Electrostatic Nature of Carbonyl Hydrogen-Bonding Interactions Using IR-NMR Correlations. *J. Phys. Chem. Lett.* **2014**, *5*, 3211−3215.

(34) Webb, L. J.; Boxer, S. G. Electrostatic Fields near the Active Site of Human Aldose Reductase: 1. New Inhibitors and Vibrational Stark Effect Measurements†. *Biochemistry* **2008**, *47*, 1588−1598.

(35) Fafarman, A. T.; Boxer, S. G. Nitrile Bonds as Infrared Probes of Electrostatics in Ribonuclease S. *J. Phys. Chem. B* **2010**, *114*, 13536−13544.

(36) Fafarman, A. T.; Sigala, P. A.; Schwans, J. P.; Fenn, T. D.; Herschlag, D.; Boxer, S. G. Quantitative, Directional Measurement of Electric Field Heterogeneity in the Active Site of Ketosteroid Isomerase. *Proc. Natl. Acad. Sci. U. S. A.* **2012**, *109*, E299−E308.

(37) Lindquist, B. A.; Furse, K. E.; Corcelli, S. A. Nitrile Groups as Vibrational Probes of Biomolecular Structure and Dynamics: An Overview. *Phys. Chem. Chem. Phys.* **2009**, *11*, 8119−8132.

(38) Dalosto, S. D.; Vanderkooi, J. M.; Sharp, K. A. Vibrational Stark Effects on Carbonyl, Nitrile, and Nitrosyl Compounds Including Heme Ligands, CO, CN, and NO, Studied with Density Functional Theory. *J. Phys. Chem. B* **2004**, *108*, 6450−6457.

(39) Getahun, Z.; Huang, C.-Y.; Wang, T.; De León, B.; DeGrado, W. F.; Gai, F. Using Nitrile-Derivatized Amino Acids as Infrared Probes of Local Environment. *J. Am. Chem. Soc.* **2003**, *125*, 405−411.

(40) Fafarman, A. T.; Sigala, P. A.; Herschlag, D.; Boxer, S. G. Decomposition of Vibrational Shifts of Nitriles into Electrostatic and Hydrogen-Bonding Effects. *J. Am. Chem. Soc.* **2010**, *132*, 12811−12813.

DOI: 10.1021/acs.jpcb.6b02732
J. Phys. Chem. B 2016, 120, 4034−4046

(41) Fleming, F. F.; Yao, L.; Ravikumar, P. C.; Funk, L.; Shook, B. C. Nitrile-Containing Pharmaceuticals: Efficacious Roles of the Nitrile Pharmacophore. *J. Med. Chem.* **2010**, *53*, 7902−7917.
(42) Bagchi, S.; Boxer, S. G.; Fayer, M. D.; Ribonuclease, S. Dynamics Measured Using a Nitrile Label with 2D IR Vibrational Echo Spectroscopy. *J. Phys. Chem. B* **2012**, *116*, 4034−4042.
(43) Urbanek, D. C.; Vorobyev, D. Y.; Serrano, A. L.; Gai, F.; Hochstrasser, R. M. The Two-Dimensional Vibrational Echo of a Nitrile Probe of the Villin HP35 Protein. *J. Phys. Chem. Lett.* **2010**, *1*, 3311−3315.
(44) Levinson, N. M.; Boxer, S. G. A Conserved Water-Mediated Hydrogen Bond Network Defines Bosutinib's Kinase Selectivity. *Nat. Chem. Biol.* **2013**, *10*, 127−132.
(45) Aschaffenburg, D. J.; Moog, R. S. Probing Hydrogen Bonding Environments: Solvatochromic Effects on the CN Vibration of Benzonitrile. *J. Phys. Chem. B* **2009**, *113*, 12736−12743.
(46) Maienschein-Cline, M. G.; Londergan, C. H. The CN Stretching Band of Aliphatic Thiocyanate Is Sensitive to Solvent Dynamics and Specific Solvation. *J. Phys. Chem. A* **2007**, *111*, 10020−10025.
(47) Choi, J.-H.; Oh, K.-I.; Lee, H.; Lee, C.; Cho, M. Nitrile and Thiocyanate IR Probes: Quantum Chemistry Calculation Studies and Multivariate Least-Square Fitting Analysis. *J. Chem. Phys.* **2008**, *128*, 154504.
(48) Choi, J.-H.; Cho, M. Vibrational Solvatochromism and Electrochromism of Infrared Probe Molecules Containing C Equivalent to O, C Equivalent to N, C═O, or C-F Vibrational Chromophore. *J. Chem. Phys.* **2011**, *134*, 154513.
(49) Lindquist, B. A.; Corcelli, S. A. Nitrile Groups as Vibrational Probes: Calculations of the C≡N Infrared Absorption Line Shape of Acetonitrile in Water and Tetrahydrofuran. *J. Phys. Chem. B* **2008**, *112*, 6301−6303.
(50) Eaton, G.; Penanunez, A. S.; Symons, M. C. R. Solvation of Cyanoalkanes CH_3CN and $(CH_3)_3CCN$ - an Infrared and Nuclear Magnetic-Resonance Study. *J. Chem. Soc., Faraday Trans. 1* **1988**, *84*, 2181−2193.
(51) Purcell, K. F.; Drago, R. S. Studies of the Bonding in Acetonitrile Adducts1. *J. Am. Chem. Soc.* **1966**, *88*, 919−924.
(52) Bischak, C. G.; Longhi, S.; Snead, D. M.; Costanzo, S.; Terrer, E.; Londergan, C. H. Probing Structural Transitions in the Intrinsically Disordered C-Terminal Domain of the Measles Virus Nucleoprotein by Vibrational Spectroscopy of Cyanylated Cysteines. *Biophys. J.* **2010**, *99*, 1676−1683.
(53) Tucker, M. J.; Getahun, Z.; Nanda, V.; DeGrado, W. F.; Gai, F. A New Method for Determining the Local Environment and Orientation of Individual Side Chains of Membrane-Binding Peptides. *J. Am. Chem. Soc.* **2004**, *126*, 5078−5079.
(54) Alfieri, K. N.; Vienneau, A. R.; Londergan, C. H. Using Infrared Spectroscopy of Cyanylated Cysteine to Map the Membrane Binding Structure and Orientation of the Hybrid Antimicrobial Peptide Cm15. *Biochemistry* **2011**, *50*, 11097−11108.
(55) Hess, B.; Kutzner, C.; van der Spoel, D.; Lindahl, E. Gromacs 4: Algorithms for Highly Efficient, Load-Balanced, and Scalable Molecular Simulation. *J. Chem. Theory Comput.* **2008**, *4*, 435−447.
(56) Wang, J. M.; Wolf, R. M.; Caldwell, J. W.; Kollman, P. A.; Case, D. A. Development and Testing of a General Amber Force Field. *J. Comput. Chem.* **2004**, *25*, 1157−1174.
(57) van der Spoel, D.; van Maaren, P. J.; Caleman, C. Gromacs Molecule & Liquid Database. *Bioinformatics* **2012**, *28*, 752−753.
(58) Caleman, C.; van Maaren, P. J.; Hong, M.; Hub, J. S.; Costa, L. T.; van der Spoel, D. Force Field Benchmark of Organic Liquids: Density, Enthalpy of Vaporization, Heat Capacities, Surface Tension, Isothermal Compressibility, Volumetric Expansion Coefficient, and Dielectric Constant. *J. Chem. Theory Comput.* **2012**, *8*, 61−74.
(59) Vorobyov, I.; Anisimov, V. M.; Greene, S.; Venable, R. M.; Moser, A.; Pastor, R. W.; MacKerell, A. D., Jr. Additive and Classical Drude Polarizable Force Fields for Linear and Cyclic Ethers. *J. Chem. Theory Comput.* **2007**, *3*, 1120−1133.
(60) Smith, M. D.; Mostofian, B.; Petridis, L.; Cheng, X.; Smith, J. C. Molecular Driving Forces Behind the Tetrahydrofuran-Water Miscibility Gap. *J. Phys. Chem. B* **2016**, *120*, 740−747.
(61) Lindorff-Larsen, K.; Piana, S.; Palmo, K.; Maragakis, P.; Klepeis, J. L.; Dror, R. O.; shaw, D. E. Improved Side-Chain Torsion Potentials for the Amber ff99sb Protein Force Field. *Proteins: Struct., Funct., Genet.* **2010**, *78*, 1950−1958.
(62) Jorgensen, W. L.; Chandrasekhar, J.; Madura, J. D.; Impey, R. W.; Klein, M. L. Comparison of Simple Potential Functions for Simulating Liquid Water. *J. Chem. Phys.* **1983**, *79*, 926−935.
(63) Bussi, G.; Donadio, D.; Parrinello, M. Canonical Sampling through Velocity Rescaling. *J. Chem. Phys.* **2007**, *126*, 01410110.1063/1.2408420
(64) Parrinello, M.; Rahman, A. Polymorphic Transitions in Single Crystals: A New Molecular Dynamics Method. *J. Appl. Phys.* **1981**, *52*, 7182−7190.
(65) Eaton, G.; Penanunez, A. S.; Symons, M. C. R.; Ferrario, M.; McDonald, I. R. Spectroscopic and Molecular-Dynamics Studies of Solvation of Cyanomethane and Cyanide Ions. *Faraday Discuss. Chem. Soc.* **1988**, *85*, 237−253.
(66) Fawcett, W. R.; Liu, G. J.; Kessler, T. E. Solvent-Induced Frequency-Shifts in the Infrared-Spectrum of Acetonitrile in Organic-Solvents. *J. Phys. Chem.* **1993**, *97*, 9293−9298.
(67) Malaspina, T.; Fileti, E. E.; Riveros, J. M.; Canuto, S. Ab Initio Study of the Isomeric Equilibrium of the $HCN\cdots H_2O$ and $H_2O\cdots HCN$ Hydrogen-Bonded Clusters. *J. Phys. Chem. A* **2006**, *110*, 10303−10308.
(68) Reimers, J. R.; Hall, L. E. The Solvation of Acetonitrile. *J. Am. Chem. Soc.* **1999**, *121*, 3730−3744.
(69) Reimers, J. R.; Zeng, J.; Hush, N. S. Vibrational Stark Spectroscopy 0.2. Application to the CN Stretch in HCN and Acetonitrile. *J. Phys. Chem.* **1996**, *100*, 1498−1504.
(70) Fried, S. D.; Wang, L.-P.; Boxer, S. G.; Ren, P.; Pande, V. S. Calculations of the Electric Fields in Liquid Solutions. *J. Phys. Chem. B* **2013**, *117*, 16236−16248.
(71) Levinson, N. M.; Fried, S. D.; Boxer, S. G. Solvent-Induced Infrared Frequency Shifts in Aromatic Nitriles Are Quantitatively Described by the Vibrational Stark Effect. *J. Phys. Chem. B* **2012**, *116*, 10470−10476.
(72) Kashid, S. M.; Jin, G. Y.; Bagchi, S.; Kim, Y. S. Cosolvent Effects on Solute-Solvent Hydrogen-Bond Dynamics: Ultrafast 2D-IR Investigations. *J. Phys. Chem. B* **2015**, *119*, 15334−15343.
(73) Pazos, I. M.; Gai, F. Solute's Perspective on How Trimethylamine Oxide, Urea, and Guanidine Hydrochloride Affect Water's Hydrogen Bonding Ability. *J. Phys. Chem. B* **2012**, *116*, 12473−12478.
(74) Jo, H.; Culik, R. M.; Korendovych, I. V.; DeGrado, W. F.; Gai, F. Selective Incorporation of Nitrile-Based Infrared Probes into Proteins Via Cysteine Alkylation. *Biochemistry* **2010**, *49*, 10354−10356.

DOI: 10.1021/acs.jpcb.6b02732
J. Phys. Chem. B 2016, 120, 4034−4046